

# SOME GEOMETRICAL RELATIONS IN DISLOCATED CRYSTALS\*

J. F. NYE†

When a single crystal deforms by glide which is unevenly distributed over the glide surfaces the lattice becomes curved. The constant feature of distortion by glide on a single set of planes is that the orthogonal trajectories of the deformed glide planes (the  $c$ -axes in hexagonal metals) are straight lines. This leads to the conclusion that in polygonisation experiments on single hexagonal metal crystals the polygon walls are planes, while the glide planes are deformed into cylinders whose sections are the involutes of a single curve. The analysis explains West's observation that the  $c$ -axes in bent crystals of corundum are straight lines. For double glide on two orthogonal sets of planes there is a complete analogy between the geometrical properties of the distorted glide planes and those of the "slip-lines" in the mathematical theory of plasticity. More general cases are discussed and formulae are derived connecting the density of dislocations with the lattice curvatures. For a three-dimensional network of dislocations the "state of dislocation" of a region is shown to be specified by a second-rank tensor, which has properties like those of a stress tensor except that it is not symmetrical.

## QUELQUES RELATIONS GÉOMÉTRIQUES DANS DES CRISTAUX DISLOQUÉS

Quand un monocristal est déformé par glissement, qui n'est pas uniformément distribué sur les surfaces de glissement, le réseau devient courbé. La caractéristique constante de distorsion par glissement sur un seul groupe de plans est, que les trajectoires orthogonales des plans de glissement déformés (les axes- $c$  dans les métaux hexagonaux) sont des droites. Ceci conduit à la conclusion, que dans les essais de polygonisation sur des monocristaux des métaux hexagonaux, les faces des polygones sont planes, alors que les plans de glissement sont déformés en des cylindres, dont les sections sont des développantes d'une seule courbe. L'analyse explique l'observation de West, que les axes- $c$  dans des cristaux fléchis de corindon sont des droites. Pour le glissement double sur deux groupes orthogonaux de plans il y a une analogie complète entre les propriétés géométriques des plans de glissement déformés et celles des lignes de glissement dans la théorie mathématique de la plasticité. Des cas plus généraux sont discutés et des formules joignant la densité des dislocations aux courbures du réseau sont déduites. Il est montré que pour un réseau de dislocations à trois dimensions "l'état de dislocation" d'une région est spécifié par un tenseur de second rang, qui a des propriétés semblables à celles du tenseur de tension, à l'exception du fait, qu'il n'est pas symétrique.

## EINIGE GEOMETRISCHE BEZIEHUNGEN IN VERFORMTEN KRISTALLEN

Wenn Einkristalle durch Gleitung verformt werden, und die Gleitung sich ungleichmässig über die Gleitebenen verteilt, dann wird das Kristallgitter "verbogen." Eine der immer wiederkehrenden Begleiterscheinungen der Verformung durch Gleitung im Fall einer einzigen Translationsebene ist, dass die Orthogonaltrajektorien der verformten Gleitebenen (in hexagonalen Metallen die  $c$ -Achsen) Geraden sind. Daraus kann man schliessen, dass in Polygonisationsexperimenten an hexagonalen Einkristallen die Wände der Polygone Ebenen sind, während sich die Gleitebenen zu Zylindern verformt haben, deren Schnitte die Evoluten einer einzigen Kurve sind. Diese Analyse erklärt die Beobachtung von West, dass die  $c$ -Achsen von "gebogenen" Korund Kristallen Geraden sind. Im Falle einer doppelten Gleitung auf zwei auf einander senkrechten Gleitebenen besteht eine völlige Analogie zwischen den geometrischen Eigenschaften der verformten Gleitebenen und den "Gleitlinien" in der mathematischen Theorie der Plastizität. Allgemeine Fälle werden diskutiert und Formeln abgeleitet, die die Dichte der Versetzungen mit der Biegung des Gitters verknüpft. Es wird gezeigt, dass in einem dreidimensionalen Netzwerk von Versetzungen der "Versetzungszustand" eines Bereiches als Tensor zweiter Ordnung dargestellt werden kann, dessen Eigenschaften denen des Spannungstensors ähnlich sind, der jedoch nicht symmetrisch ist.

## 1. Introduction

Suppose that a single crystal deforms by slip on a single set of parallel planes in such a way that the amount of slip is unevenly distributed over the slip planes. It may be asked: What possible geometrical forms can the slip planes take? This is a question that arises, for example, when a single crystal wire of zinc is bent plastically to study the phenomenon of polygonisation [1]. We do not deal in this paper with the curvatures on an atomic scale but only with the average curvatures over distances large compared with  $d$ , the dislocation spacing.

If the distribution of dislocations could be prescribed arbitrarily, there would be no limitation on the curvatures of the glide planes. An arbitrary distribution of dislocations, however, gives a large-scale distribution of internal stress. As an extreme example of this, if one calculates the stress at a given point due to a uniform array of positive edge dislocations one finds that the stress can increase to infinity as the array becomes infinite in extent. We show here from geometrical considerations that it is possible to have non-uniform distributions of dislocations that do not give accumulating stresses of this sort. Such arrays correspond to minimum strain energy configurations. In them the residual stresses average out over distances large compared to  $d$ . This property of the arrays may be stated

\*Received November 7, 1952.

†Bell Telephone Laboratories, Murray Hill, New Jersey, U.S.A.

precisely as follows: (A) If a path is constructed through "good" crystal in the sense of Frank [2] from successive lattice translation vectors, the length  $l$  of any section of the path is equal to the undistorted length, provided  $l \gg d$ . The *shape* of the path will of course be changed by the distortion. The significance of assumption (A) is easier to appreciate after the analysis that follows from it has been read.

When real crystals are distorted plastically they do in fact contain large-scale distributions of residual strains, which contribute to the lattice curvature. However, the larger the amount of plastic deformation the smaller, relatively speaking, will be this contribution to the curvature; moreover, when a distorted crystal is annealed the large-scale distributions of residual strains may be expected to disappear, while the lattice curvature will still remain. In this analysis we neglect entirely the curvature attributable to the large-scale distributions of strain.

In §§2, 3, 4 we discuss single glide. This leads to the consideration of more general cases where multiple slip occurs, and then in §8 we turn to the most general problem: the curvatures of a crystal lattice produced by a three-dimensional network of dislocations.

## 2. Single Glide: Two-Dimensional Case

It follows from assumption (A) that in single glide the distance between any two successive glide surfaces, measured along their orthogonal trajectories, is the same at all points. Consider first a two-dimensional case (Figure 1).  $S_1$  is the trace of a

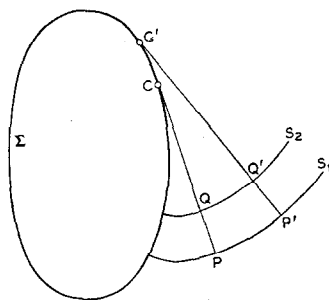


FIGURE 1. Single glide: two-dimensional case. The glide surfaces  $S_1$  and  $S_2$  are both involutes of  $\Sigma$ .

cylindrical glide surface, whose centre of curvature at  $P$  is  $C$ . As  $P$  moves along  $S_1$  the locus of  $C$  is  $\Sigma$ , the evolute of  $S_1$ .  $S_1$  can be generated by unwrapping a taut string wound round  $\Sigma$  and noting the locus of a given point  $P$ . Any other point  $Q$  on the string will sweep out a curve  $S_2$ , and, since  $PQ$  is fixed,  $S_2$  evidently satisfies the condition for being

another glide surface. (For the sake of rigour we should also remark that it may be shown that when  $PQ$  is a small element,  $S_2$  is the *only* surface lying at a fixed distance  $PQ$  from  $S_1$  measured along the orthogonal trajectories. It then follows that the same result is true for  $PQ$  finite. Huygens' construction in optics is somewhat analogous.) The glide surfaces are thus the involutes of  $\Sigma$ , which might be called the *generating curve* for the deformation. If the generating curve and its position in relation to the crystal are given, the deformation is completely specified. (The sense of the generating curve must also be given.)

The construction shows that the orthogonal trajectories of the glide planes, which were straight lines before the deformation, are also straight lines afterwards. They all have the same crystallographic direction, the  $c$ -axis in hexagonal crystals, although they are not parallel. Now, if a crystal is heated and made to polygonise [1] after a distortion of this type, it has been shown theoretically that the dislocation walls should form at right angles to the glide planes, for that is the position of lowest energy. Our construction shows that, apart from elastic strains, the traces of the walls will theoretically be strictly straight lines, even on a macroscopic scale. Thus, for example, when a hexagonal crystal is bent by basal glide so that the plane of bending contains its  $c$ -axis and one of the basal glide directions, the glide planes will deform into cylinders with parallel generators and the polygon walls will be planes. We shall call this case *plane bending*.

If the shape of any one glide surface, say  $S_1$ , is given, successive glide surfaces can be constructed on each side of it by drawing the normals to  $S_1$  and connecting points at equal distances from  $S_1$ . However, when a point is at the same distance, measured along the normal to  $S_1$ , from more than one point of  $S_1$  the construction becomes ambiguous. Such points are associated with a cusp on the generating curve. Physically, what has happened here is that flexural glide has become concentrated into a sharp kink. Figure 2 shows an instance of this.  $ABC$  is the generating curve with a cusp at  $B$ . In the area to the right of  $DBA$  the glide surfaces can be constructed by imagining a taut string to be unwrapped from the branch  $BA$ . Each point on the string sweeps out a glide surface. In the area to the left of  $DBC$  the glide surfaces can be similarly constructed by using the branch  $BC$ . There is thus an ambiguity in the area within  $ABC$ . The ambiguity is resolved in the following way. Let  $EF = GH$ , where  $EF$  and  $GH$  are normals to the glide surfaces.

Let the glide surface through  $F$ , constructed with branch  $BC$ , meet the glide surface through  $H$ , constructed with the branch  $BA$ , at the point  $J$ .  $J$  will then mark a sharp corner on the glide surface and the locus of  $J$ , shown by the broken line, will be a kink surface. It may be noted that the kink surface is not, in general, a plane.

The form of the glide surfaces in general represents a certain spatial distribution of edge dislocations of like sign. (Close pairs of dislocations of

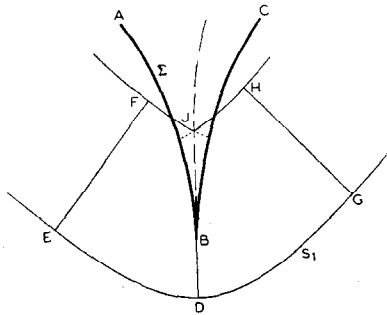


FIGURE 2. The effect of a cusp in the generating curve. Flexural glide becomes concentrated into a sharp kink.

opposite sign produce no curvature and so are irrelevant to the present analysis.) If we look at the evolute construction in terms of dislocations we see that we have found, effectively, the distribution of least strain energy for any given base distribution along a certain part of the surface  $S_1$ .

As mentioned in §1, this approach avoids any difficulties with infinite stresses that might be caused by having an infinite array of dislocations. The method of construction automatically adjusts the stresses so that they do not accumulate, and when the density of dislocations necessary to achieve this becomes infinite (on  $\Sigma$ ) the array naturally terminates. The evolute construction focusses attention on the avoidance of stresses *normal* to the glide planes, but it will be seen that it is the avoidance of *other* stresses that determines the curvature.

Let  $n$  be the number of excess dislocations of one sign per unit area and  $\mathbf{b}$  their Burgers vector. Then if we take a square Burgers circuit [2] of unit area, as shown in Figure 3, the closure failure is  $n\mathbf{b}$  and,

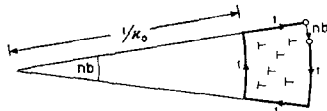


FIGURE 3. The curvature of the glide planes produced by  $n$  edge dislocations of the same sign in unit area is  $n\mathbf{b}$ .

by hypothesis, there is no elastic stretching of the circuit. The curvature  $\kappa_0$  of the glide planes in this region is therefore given by

$$(1) \quad \kappa_0 = n\mathbf{b}$$

where  $b = |\mathbf{b}|$ . Thus, on  $PC$  in Figure 1,  $n$  is inversely proportional to the distance from  $C$ . We may notice that if  $b \rightarrow 0$  and  $n \rightarrow \infty$  in such a way that  $nb$  is constant, the strain energy  $E \rightarrow 0$  but the curvature remains unchanged. Our analysis can only cover continuously varying distributions of dislocations and for this reason it cannot predict the decrease of strain energy that accompanies polygonisation. It may be noticed, however, that the above distribution ensures that when the crystal polygonises the number of dislocations per unit length is a constant in any given polygon wall.

It is a simple matter to calculate the curvature of any other lattice plane in the zone parallel to the dislocation lines. In Figure 4a,  $ABCD$  is a small element bounded by glide planes,  $AB$  and  $DC$ , and their normals. Let  $\phi_A, \phi_B, \dots$  denote the orientation of the lattice at  $A, B, \dots$  measured anti-clockwise from some fixed orientation. Then the curvature of the lattice plane  $AC$ , which makes an angle  $\theta$  with  $AB$ , is

$$(2) \quad \kappa = \frac{\phi_C - \phi_A}{AC} = \frac{\phi_B - \phi_A}{AC} = \frac{\phi_B - \phi_A}{AB} \cos \theta = \kappa_0 \cos \theta$$

or

$$\kappa = nb \cos \theta.$$

Thus, the curvature of any lattice plane parallel to the edge dislocation lines is equal to the component of  $n\mathbf{b}$  parallel to the plane. The curvature of the lattice

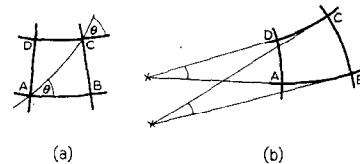


FIGURE 4. Curvatures produced by glide on (a) a single set of planes and (b) two orthogonal sets of planes, illustrating the relation  $\phi_C - \phi_B = \phi_D - \phi_A$ .

plane  $AC$  is to be distinguished from the curvature of a line inscribed on the crystal before deformation at the same angle  $\theta$  to  $AB$ . Such a line changes its orientation relative to the crystal during the deformation, and after deformation different parts of the line will, in general, be in different crystallographic directions.

We turn now to a special case.

### 3. Special Case of Uniform Plane Bending

If plane bending takes place uniformly about an axis  $O$  (Figure 5a), the generating curve  $\Sigma$  is a circle, of radius  $a$  and centre  $O$ . The orthogonal trajectories to the glide planes (the  $c$ -axes for hexagonal metal crystals) are straight lines and the

glide planes are the involutes of the circle. Using the notation that  $r$  is the radius vector to any point  $P$  (Figure 5b),  $r = r_0$  is the neutral plane,  $\chi$  is the angle of intersection of the glide planes with the fibre ( $r = \text{constant}$ ) through  $P$ , and  $\chi_0$  is the

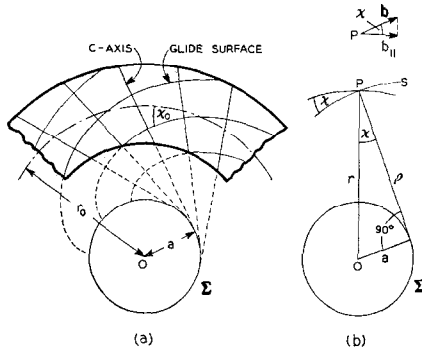


FIGURE 5. Uniform plane bending of a rod by single glide. The glide planes are the involutes of a circle, and the glide plane normals, the  $c$ -axes in hexagonal crystals, are straight lines.

angle of intersection of the glide planes with the neutral plane, we have the relations,

$$r \sin \chi = r_0 \sin \chi_0 = a; \quad \rho = r \cos \chi = \sqrt{r^2 - a^2}.$$

The same results may be obtained by noting that, after bending, the length  $l$  of a fibre which was originally of length  $l_0$  is given by

$$\frac{l}{l_0} = \frac{r}{r_0}.$$

On the other hand, the change in lattice orientation caused by this extension is expressed by [3]

$$\frac{l}{l_0} = \frac{\sin \chi_0}{\sin \chi}.$$

Hence  $r \sin \chi = r_0 \sin \chi_0 = \text{constant}$ , as before.

The radial distribution of the excess dislocation density is, from equation (1),

$$n = \frac{1}{b \sqrt{r^2 - a^2}};$$

or, more simply,

$$n = \frac{1}{b_p r},$$

where  $b_p$  is the component of  $b$  parallel to the neutral plane.

The circle  $r = a$  corresponds to a compression sufficient to turn the glide planes to a position at right angles to the fibres; it also corresponds to an infinitely high density of dislocations. If the rod is bent in such a way that the neutral plane remains fixed within it, this imposes a limit to the curvature that can be applied. By using the fact that the volume is unchanged by the deformation it is easy

to show that, when the innermost fibre is of radius  $a$ ,

$$a^2 = r_0(r_0 - 2\delta)$$

where  $\delta$  is the distance between the innermost fibre and the neutral plane *before* deformation. Using the relation  $a = r_0 \sin \chi_0$  we find the minimum radii of curvature of the neutral plane and the innermost fibre respectively,

$$(3) \quad r_0 = \frac{2\delta}{\cos^2 \chi_0}, \quad a = \frac{2\delta \sin \chi_0}{\cos^2 \chi_0}.$$

In an actual experiment an attempt to bend a rod to a smaller radius than is given by these equations would result in an inward shift of the neutral plane relative to the rod. The bending would be accomplished, in fact, by a combination of bending with extension. Our formulae are independent of the history of the bending and of whether or not it is combined with extension or compression.  $r_0$  refers always to the fibre that at the end of the deformation is found to be unchanged in length; on it,  $\chi = \chi_0$ . Formula (3) shows that, for a given  $\chi_0$ , we can make  $a$  as small as we like by simply choosing  $\delta$  small enough.

If transverse straight lines at right angles to the neutral axis were ruled on the crystal before bending, they would become curved. The calculation of their shape in polar coordinates is straightforward but tedious. The result is given in Appendix A and Figure 10.

#### 4. Experimental Verification

We have seen that in plane bending by basal glide in a hexagonal crystal, the crystallographic planes containing the  $c$ -axis and the axis of bending remain plane in spite of the bending. We may note that this does not imply that the corresponding X-ray reflexions will be free from asterism, because successive reflecting planes are not parallel. However, with a transparent crystal the extinction directions between crossed nicols can be used to show up the effect. This has been done by West [4] with single crystals of corundum (trigonal). He found as an experimental fact, without explanation, that, in crystals bent round into a loop and a U-shape, "the  $c$ -axis through any point remains a straight line even to the boundaries of the rod." He went on to deduce that the glide planes in the uniformly bent parts were the involutes of a circle, as we saw in the last section. It may be concluded that these corundum crystals had deformed by single glide. Double glide would in general give a

different distribution of lattice rotation, as will appear in the next sections.

### 5. Double Orthogonal Glide: Two-Dimensional Case

We now generalise the problem of §2 by allowing further slip to take place on the set of planes at right angles to the first set. Both slip directions are taken to be in the plane of the diagram (Figures 4a, b) and, as before, we only consider edge-type dislocations running perpendicular to the plane of the diagram. Rock salt is an example of a crystal that could deform in this way.

Let Figure 4a now show a finite curvilinear quadrilateral bounded by slip-lines after slip has occurred on the first set of planes,  $AB$ ,  $DC$ , but before it has occurred on the second set  $AD$ ,  $BC$ . Since  $\phi_A = \phi_D$  and  $\phi_B = \phi_C$ ,

$$(4) \quad \phi_C - \phi_D = \phi_B - \phi_A.$$

Now let slip take place on the second set of planes (Figure 4b). This produces additional curvatures but it is easily proved that it will not affect the curvature of  $AB$  (for instance, by drawing a Burgers

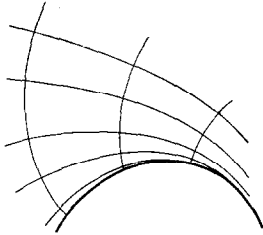


FIGURE 6. Glide on two sets of orthogonal planes.

circuit after the manner of Figure 3). Therefore, since  $AB$  is not altered in length,  $\phi_B - \phi_A$  is unaltered by the second slip. Similarly,  $\phi_C - \phi_D$  is unaltered. Hence relation (4) continues to hold after the second slip. Rearranging the terms gives

$$\phi_C - \phi_B = \phi_D - \phi_A.$$

We thus find that *the lattice rotation between two given slip-lines of one family where they are cut by a slip-line of the other family is constant along their length.*

Let  $AB$  and  $AD$  in Figure 4b now be infinitesimal with lengths  $ds$  and  $ds'$  respectively. The radii of curvature  $\rho$  and  $\rho'$  respectively of the slip-lines through  $A$  are given by

$$\frac{1}{\rho} = \frac{\partial \phi}{\partial s}, \quad \frac{1}{\rho'} = \frac{\partial \phi}{\partial s'}.$$

From the geometry of the small quadrilateral,

$$AB - DC = AD(\phi_B - \phi_A).$$

Therefore, if  $\rho_D$  and  $\rho_A$  are values of  $\rho$  at  $D$  and  $A$ ,

$$\rho_A(\phi_B - \phi_A) - \rho_D(\phi_C - \phi_D) = AD(\phi_B - \phi_A).$$

Therefore, from equation (4),

$$\rho_A - \rho_D = AD.$$

Hence,

$$\frac{\partial \rho}{\partial s} = -1, \quad \text{or} \quad d\rho + \rho' ds = 0$$

along a line of the second set. Similarly,

$$\frac{\partial \rho'}{\partial s} = 1, \quad \text{or} \quad d\rho' - \rho ds = 0$$

along a line of the first set. This means that *as one moves along the slip-lines of one set the radius of curvature of the slip-lines of the other set changes by the distance moved.* The radius decreases as one moves towards the inside of the curves. Thus, in general, the radius of curvature eventually decreases to zero and the slip-lines that are being followed run together (Figure 6). We have already had an instance of this in the special case of single glide.

The two geometrical properties of the slip-lines or glide lines expressed above are identical with Hencky's first and second theorems in the mathematical theory of plasticity [5]. On the other hand, the "slip-lines" in that theory are quite different from the slip-lines we have been discussing. They are defined as the trajectories of maximum shear stress in the stress field, or as characteristics of the fundamental hyperbolic equations of the theory. We thus have the curious situation, a sort of mathematical pun, that not only are these two dissimilar families of curves called by the same name but they also obey the same equations.

The small arc process used in the theory of plasticity to build up the slip-line field in any finite quadrilateral  $ABCD$ , given the form of the slip-lines  $AB$  and  $AD$ , is equally applicable here.

The answer to the question, then, as to what forms the slip planes can take after glide on orthogonal planes is that they can be any families that satisfy the Hencky relations.

### 6. Multiple Glide: Two-Dimensional Case

Still confining attention to the two-dimensional case of an array of parallel edge dislocations we may now consider the effect of glide on any number of different planes. If in unit area there are  $n_r$  dislocations with Burgers vector  $\mathbf{b}_r$ , the curvature of any lattice plane parallel to the dislocation lines is obtained (§2) by summing the components of the vectors  $n_r \mathbf{b}_r$  in the direction of the plane—which is the same as taking the component of the vector

$$\sum_r n_r \mathbf{b}_r$$

in that direction. At the point considered, therefore, the dislocations are equivalent to a set on a single plane, but of course this plane will be different, in general, for every point of the crystal, according to the ratios of the  $n_r$ .

### 7. General Three-Dimensional Case for Single Glide

In three dimensions it may be shown by similar reasoning to that of §2 that the curves orthogonal to the glide surfaces are necessarily straight lines, even for the most general type of distortion, provided only that it takes place by glide on a single set of planes. Any number of glide *directions* may operate. However, in this case, unlike the two-dimensional case, the lattice orientation is not fixed along the normal, for the lattice can and does, in general, twist about the normal. In two dimensions the centre of curvature of  $S_1$  at  $P$  (Figure 1) was the same as the centre of curvature of  $S_2$  at  $Q$  and so on, namely  $C$ . Similarly in three dimensions, all the glide surfaces intersecting a given normal share the same two centres of curvature lying on their common normal. As we follow a normal, therefore, both radii of curvature change by the distance travelled. They increase or decrease respectively according to whether we are receding from or approaching the corresponding centre of curvature. Moreover, the two principal curvature directions are preserved along a given normal. The two surfaces described by the two centres of curvature as the normal moves represent the three-dimensional analogues of the evolute of two dimensions.

For a set of parallel like dislocations of general type there are simple relations (proved in Appendix B) between their direction and the curvature they produce in their glide planes. Figure 7 shows the

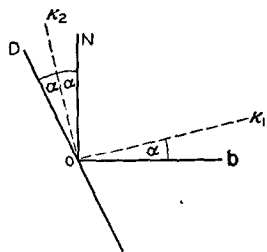


FIGURE 7. Glide on a single set of planes: three-dimensional case. The slip plane is the plane of the diagram. The principal directions of curvature bisect the angle between the dislocation lines and  $ON$ .

relations between the various directions in a glide plane. The two principal directions of curvature in the glide plane are the internal and external bisectors of the angle, of magnitude  $2\alpha$ , between the

direction,  $OD$ , of the dislocation lines and  $ON$ , the normal to  $\mathbf{b}$ . Thus, if the dislocations are pure edge,  $\alpha = 0$ , and the directions of the principal curvatures  $\kappa_1$  and  $\kappa_2$  are parallel and perpendicular to  $\mathbf{b}$ ; while if the dislocations are pure screw,  $\alpha = \pi/4$ , and  $\kappa_1$  and  $\kappa_2$  are at angles of  $\pi/4$  to  $\mathbf{b}$ . The magnitudes of the curvatures are

$$\kappa_1 = nb \cos^2 \alpha, \quad \kappa_2 = -nb \sin^2 \alpha,$$

where  $n$  is the number of dislocation lines per unit area normal to the lines. Hence

$$\kappa_1 - \kappa_2 = nb,$$

and is independent of  $\alpha$ . We also have

$$\kappa_1 + \kappa_2 = nb \cos 2\alpha = n'b$$

where  $n'$  is the number of lines per unit area taken normal to  $ON$ .

### 8. General Three-Dimensional Case

Finally we come to the most general case that falls within the scope of this type of treatment, a three-dimensional network of dislocations. As before, we consider a region of the crystal large enough for the effects of the dislocations within it to be averaged. Alternatively, we may make the distribution of dislocations continuous by letting  $b$  approach zero and increasing the number of dislocations of each kind in proportion, so as to keep the curvatures constant (cf. §2). Our aim is to find the relation between the dislocations in the region and the curvatures of the lattice that they produce.

Consider first the dislocations. They may be specified by taking Burgers circuits in different orientations and noting the closure failures (Burgers vectors). If a Burgers circuit of unit area normal to the unit vector  $l_j$  has a Burgers vector  $B_i$  (that is to say,  $B_i$  completes the circuit when it is traversed in the sense of a right-handed screw motion along  $l_j$ ) then it is shown in Appendix C that we may write

$$(5) \quad B_i = \alpha_{ij} l_j, \quad (i, j = 1, 2, 3).$$

The summation convention is to be understood. The components  $B_i$  form an axial vector. The coefficients  $\alpha_{ij}$  relate the two vectors  $B_i$  and  $l_j$  and therefore form a second-rank tensor; it specifies the "state of dislocation" of the region.

To calculate the  $\alpha_{ij}$  components for a given set of dislocations the procedure would be as follows. Suppose there are dislocations with length parallel to the unit vector  $\mathbf{r}$  and with Burgers vector  $\mathbf{b}$ . Let there be  $n$  of these dislocations crossing unit area normal to  $\mathbf{r}$ . The number crossing unit area normal to the unit vector  $\mathbf{l}$  is  $n\mathbf{r} \cdot \mathbf{l}$ . The associated

Burgers vector is  $\mathbf{b}(n\mathbf{r}\cdot\mathbf{l})$ . Hence, in suffix notation,

$$B_i = b_i(n r_j l_j)$$

and, from equation (5),

$$\alpha_{ij} = n b_i r_j.$$

If there are other sets of dislocations present with different values of  $n$ ,  $\mathbf{b}$  and  $\mathbf{r}$ , the total  $\alpha_{ij}$  is obtained by summing the values of  $n b_i r_j$  for all the sets.

The form of  $\alpha_{ij}$  implies that, so far as curvatures are concerned, any state of dislocation can be produced by combining nine sets of dislocations with their lengths and their Burgers vectors arranged parallel and perpendicular to the coordinate

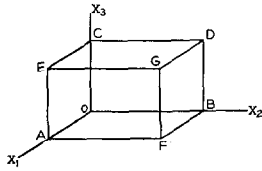


FIGURE 9

axes. The three terms of the leading diagonal represent pure screw dislocations and the six cross-terms represent the six possible types of pure edge dislocations. Alternatively, by combining the three types of dislocation lines directed along each axis the general state can be regarded as produced by three perpendicular sets of dislocations of general type. Such a representation would of course only be unique for a given set of axes.

We now have to specify the curvatures of the lattice. Let  $d\phi_i$  be the small lattice rotations about the three axes, in a right-handed screw sense, associated with the displacement vector  $dx_j$ . The  $d\phi_i$  are the components of an axial vector. If we now write

$$(6) \quad d\phi_i = \kappa_{ij} dx_j$$

the coefficients  $\kappa_{ij}$  form a second-rank tensor which describes the curvature of the lattice.

In Appendix D we show that the dislocation tensor  $\alpha_{ij}$  is related to the curvature tensor  $\kappa_{ij}$  by the equation

$$(7) \quad \alpha_{ij} = \kappa_{ji} - \delta_{ij} \kappa_{kk} \quad (i, j, k = 1, 2, 3)$$

where  $\delta_{ij} = 1$  for  $i = j$ , and  $\delta_{ij} = 0$  for  $i \neq j$ . The reverse relation is

$$(8) \quad \kappa_{ij} = \alpha_{ji} - \frac{1}{2} \delta_{ij} \alpha_{kk}.$$

The general property of a dislocation network, that the Burgers vector is conserved along any dislocation line and at a node, is associated with a corresponding theorem in the present formulation. Consider the small rectangular parallelepiped shown in Figure 9. The faces define six Burgers circuits,

and we specify that each is to be taken in the direction associated with the outward normal to the face. We now traverse all six in turn and show that the final result is that we have traversed a circuit of zero area. Thus:

$$\begin{aligned} & (OCDBO + OBFAO + OAECO) \\ & + (GEAFG + GFBDG + GDCEG) \\ & = CDBFAEC + EAFBDCE = 0. \end{aligned}$$

Therefore the total Burgers vector for the six circuits is zero. Equating the components to zero and proceeding to the limit we have

$$\frac{\partial \alpha_{11}}{\partial x_1} + \frac{\partial \alpha_{12}}{\partial x_2} + \frac{\partial \alpha_{13}}{\partial x_3} = 0$$

and two similar equations. Thus, in general,

$$(9) \quad \frac{\partial \alpha_{ij}}{\partial x_j} = 0.$$

The general analysis of the tensor  $\alpha_{ij}$  is therefore formally the same as that for the tensor of mechanical stress with the one difference that  $\alpha_{ij}$  is not symmetrical; equations (9) are the analogues of the equations of equilibrium.

It is interesting to notice too the formal similarity between equations (7) and the stress-strain relations in an isotropic body,

$$\sigma_{ij} = 2\mu \epsilon_{ij} + \lambda \delta_{ij} \epsilon_{kk}$$

with  $2\mu = 1$ ,  $\lambda = -1$ ;  $\alpha_{ij}$  plays the part of the stress and  $\kappa_{ij}$  that of the strain, although, unlike these tensors  $\alpha_{ij}$  and  $\kappa_{ij}$  are not symmetrical. These values of  $\lambda$  and  $\mu$  give Young's Modulus = 2, Rigidity Modulus =  $\frac{1}{2}$ , Poisson's Ratio = 1 and Bulk Modulus =  $-\frac{2}{3}$ .

Since

$$\kappa_{ij} = \frac{\partial \phi_i}{\partial x_j}$$

we have

$$\frac{\partial \kappa_{ij}}{\partial x_k} = \frac{\partial^2 \phi_i}{\partial x_j \partial x_k} = \frac{\partial \kappa_{ik}}{\partial x_j}.$$

By substituting  $\alpha$  for  $\kappa$  from equation (8) we obtain the equations

$$(10) \quad \frac{\partial \alpha_{ji}}{\partial x_k} - \frac{\partial \alpha_{ki}}{\partial x_j} = \frac{1}{2} \left( \delta_{ij} \frac{\partial \alpha_{ll}}{\partial x_k} - \delta_{ik} \frac{\partial \alpha_{ll}}{\partial x_j} \right)$$

Of the twenty-seven possible permutations of  $i, j, k$  the equations given by those nine with  $j = k$  are trivial. Of the remaining eighteen equations, owing to the symmetry in  $j$  and  $k$ , only nine are independent. Thus there are nine independent differential equations to determine the nine independent  $\alpha_{ij}$  components.

By putting  $i = j$  or  $i = k$  in equations (10) a

little reduction shows that we recover the "equilibrium equations" (9).

By analogy with the strain energy function in elasticity it is useful to introduce, purely formally, the function

$$W = \frac{1}{2} \alpha_{ij} \kappa_{ij}.$$

Then, by differentiating and using equations (7),

$$\begin{aligned} \frac{\partial W}{\partial \kappa_{ij}} &= \frac{1}{2} \alpha_{ij} + \frac{1}{2} \frac{\partial \alpha_{kl}}{\partial \kappa_{ij}} \kappa_{kl} = \frac{1}{2} \alpha_{ij} + \frac{1}{2} \kappa_{ji} - \frac{1}{2} \delta_{ij} \kappa_{kk} \\ &= \alpha_{ij}. \end{aligned}$$

$W$  is thus a "dislocation potential." It is a function of the components of lattice curvature at any point such that its derivatives with respect to each component of curvature are each equal to the corresponding component of the state of dislocation.

## 9. Discussion

Eshelby [6], using a model described by Timoshenko, has discussed a state of internal stress which Nabarro [7] has called a continuous distribution of dislocations. That this state of dislocation is different from the one treated here may be seen by considering the case of single glide (§2). One way of arriving at our model of the process would be to suppose an unstrained body cut up into small cubes of side  $d$ . The structure is then bent by allowing sliding to take place parallel to one set of faces only of the cubes (flexural glide), the cubes themselves being unstrained. There will then be voids between the cubes. The strain of the cubes necessary to fill the voids is of order  $\kappa d$ , where  $\kappa$  is the mean curvature of the surfaces of sliding. As  $d \rightarrow 0$  with  $\kappa$  held constant, this strain  $\rightarrow 0$ . In Eshelby's model the strain does not approach zero as the cubes are made small and he is essentially concerned with a state of internal stress. The difference between our models is that we allow sliding of the cubes or other elementary pieces, as is actually produced in crystals by the movement of dislocations, while Eshelby does not.

The energy of a single dislocation at the centre of a crystal of linear dimensions  $R$  is of the general form

$$Gb^2 \ln \frac{R}{r_0},$$

where  $G$  is an elastic constant and  $r_0$  is a length of the order of atomic dimensions.\* In the arrays of dislocations considered in this paper, where stresses do not accumulate,  $R$  may be taken as the mean spacing of the dislocations, say  $n^{-\frac{1}{2}}$ , or  $(b/\kappa)^{\frac{1}{2}}$ ,

\*I am much indebted to the referee for most of the substance of the remainder of this discussion.

where  $\kappa$  is the local curvature. The strain energy in a unit volume, therefore, which contains  $n = \kappa/b$  dislocations, is of the form

$$\frac{\kappa}{b} \cdot Gb^2 \ln \left\{ \left( \frac{b}{\kappa} \right)^{\frac{1}{2}} \cdot \frac{1}{r_0} \right\}.$$

This is proportional to

$$\kappa Gb \ln \frac{b}{\kappa r_0^2} = \kappa Gb \ln \frac{m}{\kappa b},$$

where  $m = b^2/r_0^2$ , a constant that depends upon the details of the atomic arrangements on the dislocation axis. As  $b \rightarrow 0$  with  $\kappa$  constant, the energy approaches zero, as noted in §2.

The analysis of this paper is closely related to Frank's construction [8] for grain boundaries. In fact the Frank representation is essentially a surface distribution of dislocation density, or  $\alpha_{ij}$ , and, although we do not give this development here, the Frank formulation is deducible from the present analysis. Grain boundary arrays are a special case of these more general distributions, and have the characteristic in common that they represent a state of minimum energy and that the total energy is linear in the Burgers vector, or more precisely is of the general form noted above. The stability of polygonized arrays arises from the fact that the argument of the logarithmic term above really depends on the closest approach of the individual

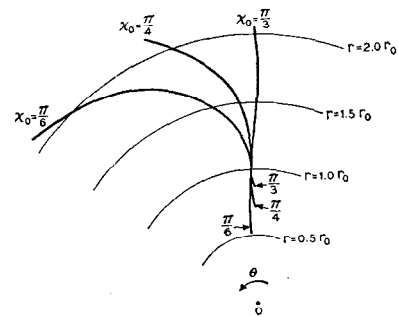


FIGURE 10. Showing the form of transverse lines after uniform plane bending of a crystal bar by single glide for three initial orientations ( $\chi_0$ ).

dislocations rather than on their average separation, given by  $n^{-\frac{1}{2}}$ . Polygonized arrays preserve the mean dislocation density, as pointed out in §2, but they achieve a smaller minimum separation and hence a smaller total energy than uniform distributions.

## Appendix A

The equations in polar coordinates of the transverse lines on the uniformly bent crystal referred to on p. 156 are, in terms of  $\chi$  as a parameter,

$$r = r_0 \sin \chi_0 \operatorname{cosec} \chi$$

$$\theta = \frac{1}{4} \sin 2\chi_0 \cot^2 \chi - \cot \chi - \chi + \text{const.}$$



The curves, which in general show a reversal of curvature, all have the same shape, different members corresponding to different values of the constant in the expression for  $\theta$ . The curves for  $\chi_0 = \pi/6, \pi/4, \pi/3$  are drawn in Figure 10. When  $0 < \chi_0 < \pi/4$ ,  $\theta$  has a maximum on the compression side at  $r = r_0 \tan \chi_0$  and a minimum at  $r = r_0$ . When  $\chi_0 = \pi/4$ ,  $r = r_0$  is a point of inflexion. When  $\pi/4 < \chi_0 < \pi/2$ ,  $r = r_0$  is a maximum and  $r = r_0 \tan \chi_0$ , on the tension side, is a minimum.

### Appendix B\*

In Figure 7 we regard the angle  $NOD = 2\alpha$  as fixed and we calculate the curvatures of the glide plane. Take a square Burgers circuit with sides of unit length whose normal lies in the plane of the figure at an angle  $\beta$  to  $OD$ . The number of dislocation lines threading the circuit is  $n \cos \beta$ . The closure failure is thus  $nb \cos \beta$ . The circuit makes an angle  $(2\alpha - \beta)$  with  $\mathbf{b}$ ; the component of the closure failure parallel to the circuit is  $nb \cos \beta \cos (2\alpha - \beta)$  therefore. This component is a maximum or minimum when  $\beta = \alpha$  and  $(\alpha + \frac{1}{2}\pi)$ , that is, when the normal to the circuit bisects the angle  $NOD$  internally and externally. These bisectors then are the two directions of principal curvature. Reference to Figure 3 shows that the curvatures themselves are the two corresponding values of  $nb \cos \beta \cos (2\alpha - \beta)$ , that is

$$\kappa_1 = nb \cos^2 \alpha \text{ and } \kappa_2 = -nb \sin^2 \alpha$$

### Appendix C\*

A proof of equations (5) is as follows. Consider the tetrahedron shown in Figure 11. Let  $ABC$  be of unit

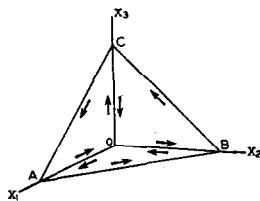


FIGURE 11

area and normal to  $l_j$ . Let a Burgers circuit of unit area normal to  $Ox_1$  have a Burgers vector with components  $(\alpha_{11}, \alpha_{21}, \alpha_{31})$ . Then the circuit  $OBCO$  has a Burgers vector  $(\alpha_{11} l_1, \alpha_{21} l_1, \alpha_{31} l_1)$ . With a similar notation  $OCAO$  has a Burgers vector  $(\alpha_{12} l_2, \alpha_{22} l_2, \alpha_{32} l_2)$  and  $OABO$  has a Burgers vector  $(\alpha_{13} l_3, \alpha_{23} l_3, \alpha_{33} l_3)$ . If we now traverse these three circuits one after the other, the arms  $OA, OB, OC$

are each traversed twice, once in each direction, and therefore cancel; we are left with the circuit  $ABCA$  whose closure failure must be the sum of the three for the separate circuits. Thus, for  $ABCA$ ,

$$B_1 = \alpha_{11} l_1 + \alpha_{12} l_2 + \alpha_{13} l_3$$

$$B_2 = \alpha_{21} l_1 + \alpha_{22} l_2 + \alpha_{23} l_3$$

$$B_3 = \alpha_{31} l_1 + \alpha_{32} l_2 + \alpha_{33} l_3$$

or, briefly,

$$(5) \quad B_i = \alpha_{ij} l_j.$$

### Appendix D†

We give here a proof of equations (7). Suppose the  $\kappa_{ij}$  are given. Take a small square Burgers circuit of unit area normal to  $Ox_1$  as shown in Figure 8. The

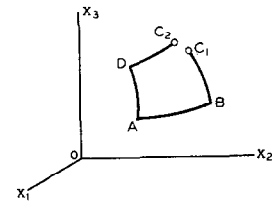


FIGURE 8

closure failure  $B_1$  is  $\vec{C_1 C_2}$ . This may be regarded as compounded of separate elements corresponding to the curvatures and twist as we traverse each arm of the circuit in turn; Figure 3 shows a special case of this. Taking  $A$  as fixed, as we move along  $\vec{AB}$ , which is parallel to  $Ox_2$ , the lattice rotations about the three axes are  $\kappa_{12}, \kappa_{22}, \kappa_{32}$ , from equation (6). By visualising the movements the resulting components of displacement of  $C_1$  can be seen to be

$$\kappa_{22} - \frac{1}{2}\kappa_{32}, -\kappa_{12}, \frac{1}{2}\kappa_{12}.$$

The displacements of  $C_1$  as we move along  $\vec{BC_1}$  are

$$\frac{1}{2}\kappa_{23}, -\frac{1}{2}\kappa_{13}, 0.$$

Similarly, as we move along  $\vec{AD}$  the displacements of  $C_2$  are.

$$\frac{1}{2}\kappa_{23} - \kappa_{33}, -\frac{1}{2}\kappa_{13}, \kappa_{13},$$

and as we move along  $\vec{DC_2}$  the displacements of  $C_2$  are

$$-\frac{1}{2}\kappa_{32}, 0, \frac{1}{2}\kappa_{12}.$$

The total closure failure  $B_i$  is then given by the difference between the displacements of  $C_1$  and  $C_2$ , thus:

$$B_1 = -(\kappa_{22} + \kappa_{33}), B_2 = \kappa_{12}, B_3 = \kappa_{13}.$$

But, from equations (5) with  $l_j = (1, 0, 0)$  we have

$$B_1 = \alpha_{11}, B_2 = \alpha_{21}, B_3 = \alpha_{31}.$$

\*See page 158.

†See page 159.

Therefore,

$$\alpha_{11} = -(\kappa_{22} + \kappa_{33}), \alpha_{21} = \kappa_{12}, \alpha_{31} = \kappa_{13},$$

and, in a similar way, by taking circuits normal to  $Ox_2$  and  $Ox_3$  we obtain

$$\alpha_{12} = \kappa_{21}, \alpha_{22} = -(\kappa_{33} + \kappa_{11}), \alpha_{32} = \kappa_{23},$$

$$\alpha_{13} = \kappa_{31}, \alpha_{23} = \kappa_{32}, \alpha_{33} = -(\kappa_{11} + \kappa_{22}).$$

Thus, in general, the relation between the  $\alpha_{ij}$  describing the state of dislocation and the  $\kappa_{ij}$  describing the curvature is

$$(7) \quad \alpha_{ij} = \kappa_{ji} - \delta_{ij} \kappa_{kk} \quad (i, j, k = 1, 2, 3)$$

where  $\delta_{ij} = 1$  for  $i = j$ , and  $\delta_{ij} = 0$  for  $i \neq j$ .

### Acknowledgments

Dr. C. D. West was kind enough to show me his paper on the corundum crystals before publication

and I am glad to acknowledge here that it suggested to me the evolute construction of §2. I am also indebted to Dr. W. M. Lomer for his comments on the manuscript.

### References

1. CAHN, R. W. J. Inst. Metals, **76** (1949) 121.
2. FRANK, F. C. Phil. Mag., **42** (1951) 809.
3. SCHMID, E. and BOAS, W. Plasticity of Crystals (London, F. A. Hughes, 1950), p. 58.
4. WEST, C. D. Paper to be submitted to J. Appl. Phys.
5. HILL, R. The Mathematical Theory of Plasticity (Oxford, University Press, 1951), p. 136.
6. ESHELBY, J. D. Phil. Trans., **A244** (1951) 87.
7. NABARRO, F. R. N. Adv. Phys., **1** (1952) 269.
8. FRANK, F. C. Plastic Deformation of Crystalline Solids (Pittsburgh Conference, 1950), p. 150.